Proceedings of the 5th International Conference on Materials Chemistry and Environmental Engineering
DOI: 10.54254/2755-2721/130/2025.19994

Gold Nanoparticle Enhanced Polyurethane Elastomer with High-Efficiency Self-healing and Potent Mechanical Property

Songqian Luo[1,a,*]

[1]*Shanghai High School International Division, Shanghai, China*
a. tonyluosq@gmail.com
**corresponding author*

Abstract: Thermoplastic polyurethanes (TPUs) are renowned for their superior mechanical properties, including elasticity, durability, and abrasion resistance, which make them indispensable in industries such as automotive, construction, and electronics. However, conventional TPUs often lack self-healing capabilities, limiting their lifespan and increasing maintenance costs. This study addresses this limitation by developing a novel TPU elastomer (PUAN-1) that incorporates gold nanoparticles (AuNPs) and disulfide bonds to enhance both mechanical strength and self-healing efficiency. The AuNPs serve as a reinforcing phase, improving the TPU's mechanical performance by strengthening the hard segments and promoting dynamic disulfide bond reformation through photothermal effects. This innovative approach enables the TPU to achieve rapid self-healing under mild conditions while maintaining excellent mechanical properties. Experimental evaluations demonstrated that PUAN-1 exhibited an ultimate tensile strength of 4.4 MPa, an elongation at break of 1165%, and a toughness of 39.7 MJ/m³, significantly outperforming conventional TPUs. Additionally, PUAN-1 displayed a high self-healing efficiency, with over 88% recovery in mechanical properties within two hours of damage. Conversely, a higher concentration of AuNPs, as in PUAN-2, was found to hinder both self-healing and mechanical performance due to restricted chain mobility and suppressed microphase separation. These findings highlight the critical balance required in optimizing AuNP content to maximize both reinforcement and flexibility. The developed TPU elastomer presents a promising candidate for applications demanding durable, self-repairing materials, such as wearable electronics, flexible sensors, and biomedical devices. This study provides valuable insights into the design of advanced TPUs that combine high mechanical robustness with effective self-healing capabilities, offering significant potential for use in dynamic and demanding environments.

Keywords: Thermoplastic polyurethanes (TPUs), self-healing, gold nanoparticles (AuNPs), disulfide bonds, mechanical property.

1. Introduction

Thermoplastic polyurethanes (TPUs) are versatile materials renowned for their outstanding mechanical properties, including elasticity, durability, and resistance to abrasion, which make them highly valuable in industries such as automotive, construction, and electronics[1, 2]. Traditionally,

DOI: 10.54254/2755-2721/130/2025.19994

TPU elastomers have been used in a range of applications, from car seats and insulation panels to electronic device housings, due to their ability to withstand wear and environmental stresses[3, 4]. However, as industrial requirements evolve, there is a growing demand for materials that not only retain superior mechanical strength but also exhibit self-healing capabilities to enhance durability and minimize maintenance costs[5]. Despite their benefits, current PU materials encounter challenges in achieving an optimal balance between mechanical robustness and self-healing efficiency. While many conventional TPUs are strong and durable, they often lack the capacity for self-repair when damaged, which can shorten their lifespan and increase the costs related to maintenance and replacement. Therefore, developing advanced TPU that integrate high mechanical performance with effective self-healing properties is essential for future industrial applications[6].

To address the demand for robust self-healing properties in TPUs, a range of methods has been developed, encompassing both intrinsic and extrinsic approaches[7, 8]. Intrinsic self-healing relies on mechanisms such as noncovalent interactions like hydrogen bonding, or reversible covalent bonding, including metal-ligand coordination and disulfide bonds[5]. In contrast, extrinsic self-healing methods involve the release of healing agents from microcapsules triggered by damage. A significant challenge for researchers is the inherent contradiction in achieving both strong mechanical properties and effective self-healing capabilities simultaneously. Developing a polymer that can efficiently self-heal while withstanding substantial mechanical stress remains a complex task[9].

Although existing techniques have shown potential in enhancing the durability and reliability of TPUs, a considerable research gap remains in balancing high mechanical strength with effective self-healing. In particular, the synergistic effects of nanoparticles combined with dynamic covalent bonds, such as disulfide bonds, within TPUs have not been thoroughly investigated. Nanoparticles with large surface areas, such as carbon nanotubes, silica nanoparticles, or gold nanoparticles (AuNPs), present promising opportunities to reinforce TPUs by improving mechanical strength through unique interactions with the polymer matrix. Further investigation into these synergies could lead to the development of advanced TPUs with both superior mechanical and self-healing properties.

This study aims to address the research gap by developing and characterizing a TPU elastomer that incorporates disulfide bonds and gold nanoparticles (AuNPs) to achieve novel mechanical and self-healing properties. The primary focus is on evaluating the mechanical strength and self-healing efficiency of the modified elastomer, as well as investigating the interactions between disulfide bonds and AuNPs within the TPU matrix. In this system, triblock copolymer diols (PCL-PEG-PCL) are used as the soft segments, isophorone diisocyanate (IPDI) as the hard segment, and bis(4-hydroxyphenyl) disulfide (BDS) as the chain extender, with the disulfide bonds in BDS playing a crucial role in enabling self-repair[10, 11]. AuNPs, recognized for their high surface area, excellent biocompatibility, and strong interaction with disulfide bonds, are pivotal in enhancing the mechanical and self-healing properties of TPUs. They can interact with disulfide bonds to form a reinforcing phase within the TPU matrix, potentially increasing mechanical strength and toughness through nanoscale interactions and effective stress distribution. Moreover, the photothermal effect of AuNPs can be utilized to enhance the self-healing process by generating localized heat that facilitates the reformation of disulfide bonds, thereby accelerating repair and improving overall self-healing efficiency. Leveraging these unique properties of AuNPs, the newly developed TPU elastomer has demonstrated impressive mechanical performance, achieving a tensile stress of 4.4 MPa, an elongation at break of 1165%, and a toughness of 39.7 MJ/m^3. These advancements highlight the potential of this next-generation elastomer to overcome current limitations of TPUs, offering superior performance characteristics for a wide range of applications.

DOI: 10.54254/2755-2721/130/2025.19994

2. Experimantal Section

2.1. Material

Polyethylene glycols (OH-PEG-OH, Mn ≈ 1000, PDI= 1.09) was purchased from Alfa Aesar Co., Ltd. ε-Caprolactone (≥ 99.9%) was purchased from Ju Ren Co., Ltd. IPDI, (≥ 99.8%) was purchased from BASF Co., Ltd. BDS (≥ 99.9%) and n-butyl titanate (TBT, ≥ 99.5%) were purchased from Aladdin Co., Ltd. Methacryloyl Chloride (≥ 99.5%) was purchased from Adamas Co., Ltd. Methacryloyl Chloride (≥ 99.5%) was purchased from Adamas Co., Ltd. AuCl (≥ 99.8%) and oleylamine (≥ 99.5%) were purchased from TCI Co., Ltd. N,N-Dimethylformamide (DMF, RG) and chloroform (RG) were purchased from Adamas Co., Ltd.

2.2. Synthesis of HO-PCL-PEG-PCL-OH

A typical method for synthesizing HO-PCL-PEG-PCL-OH is illustrated in Fig. 1. HO-PEG-OH (Mn ≈ 1050, PDI = 1.09, 50 wt.%), ε-caprolactone (50 wt.%), and n-butyl titanate (TBT, 25 ppm) were placed into a glass reaction flask equipped with a vacuum pump and an oil bath. Initially, the flask was purged with nitrogen and the mixture was stirred at 120 °C for 17 hours. This was followed by a vacuum treatment (<150 mbar) at 135 °C for an additional 3 hours. After the reaction, the product was cooled to 80°C, then filtered, packaged, and sampled for analysis. ^{1}H NMR spectroscopic data for HO-PCL-PEG-PCL-OH was shown in Fig. 2.

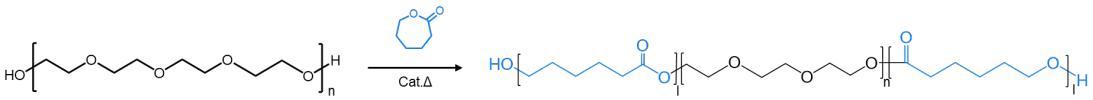

Figure 1: Schematic illustration of the synthesis of the tri-Block co-Polymer diol HO-PCL-PEG-PCL-OH.

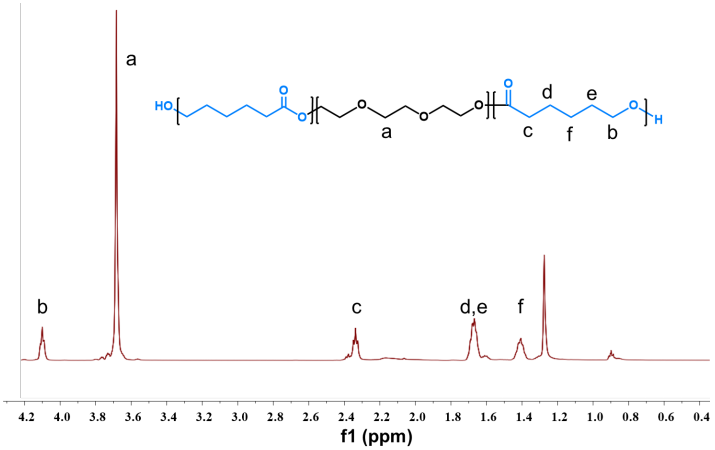

Figure 2: ^{1}H-NMR spectra of the tri-block co-polymer diols of HO-PCL-PEG-PCL in $CDCl_3$ at room temperature.

2.3. Synthesis of AuNP

0.01 g AuCl (or AuBr as a substitute) was mixed with certain volumes of oleylamine and chloroform in a glass vial of 20 mL. The solution was agitated for two minutes to dissolve AuCl (or AuBr) in the solvent. A clear solution of AuI complex should be formed. The solution was heated to 60 °C with an oil bath, stirred, and reacted to form gold nanoparticles. Upon completion, the nanoparticles are filtered with 5 mL acetone, followed by centrifugation (3900 rpm, 5 min). The nanoparticles were dispersed with 2 mL chloroform, washed with 5 mL acetone, and re-dispersed in 2 mL chloroform.

DOI: 10.54254/2755-2721/130/2025.19994

Synthesis of nanoparticles with octadecylamine followed the same procedure. TEM images of the AuNPs was shown in Fig. 3.

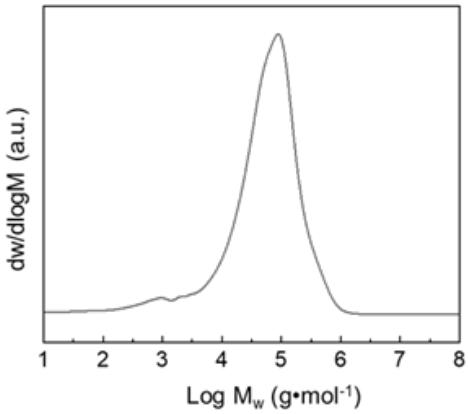

Figure 3: GPC charts of the macromolecular initiators and tri-block co-polymer diols in DMF at room temperature.

2.4. Synthesis of Prepolymer and TPU

To begin, 72 wt.% of IPDI was added to a 500-mL three-necked round-bottom flask. The flask was then maintained under a nitrogen atmosphere, and the mixture was stirred at 55 °C. Next, 28 wt.% of macropolyol (acting as soft segments) was introduced into the flask, where it was heated to 85°C for 2 hours to form the prepolymers. Afterward, the prepolymers were cooled to 60°C, then packaged, sampled, and characterized. Subsequently, TPU was synthesized from these prepolymers. The prepolymers were preheated to 80 °C for at least 30 minutes to lower their viscosity. Once preheated, 91.0 wt.% of these prepolymers were mixed with 9.0 wt.% BDS was dissolved in DMF using a FlackTek SpeedMixer set to 2500 rpm for 1 minute. The prepared mixture was poured into molds preheated to 110 °C, maintained for 1 hour, then allowed to cool to below 60 °C. The PU samples were carefully removed from the molds and underwent post-curing at 110 °C for a minimum of 16 hours. The detailed synthesis steps of TPU are depicted in Fig. 4.

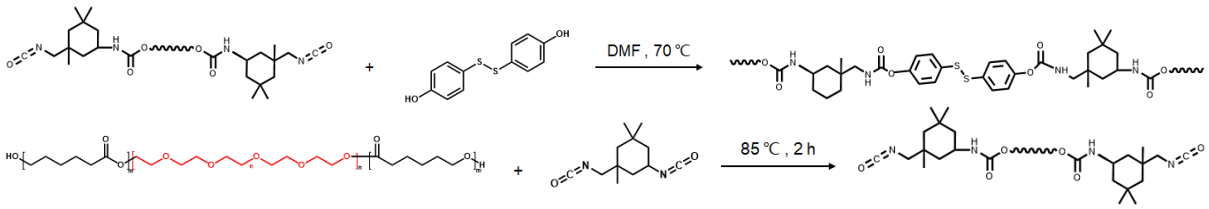

Figure 4: Schematic illustration of the synthesis of TPU.

2.5. Preparaton of PU, PUAG-1 and PUAG-2

Three separate groups of TPU were prepared: melted TPU and the solution was mixed with a ratio of 2g TPU to 0, 400, and 1600μL of the AuNP solution (the three groups were named PU, PUAN-1, and PUAN-2 during testing).

2.6. Polymer Characterization

Gel Permeation Chromatography (GPC). The molecular weight (M_w) and polydispersity index (PDI) of the TPU was measured at 30 °C. DMF served as the elution phase for TPU, with a flow rate set at 1.0 mL/min. The system was calibrated using narrow polyethylene oxide standards, which covered a molecular weight range from 550 to 100,000 g/mol. The TPUs were analyzed using Total internal

DOI: 10.54254/2755-2721/130/2025.19994

Reflection Infrared Spectroscopy (ATR-IR) spectroscopy (Thermofisher Nicolet 6700) equipped with a KRS-5 crystal that has a refractive index of 2.4 and an incidence angle of 45°. The instrument operated with a resolution of 2.0 cm^{-1}, and each sample underwent 64 scans for accurate characterization. Tensile Experiments was conducted on Instron 5966 uniaxial tensile tester equipped with a 10 N load cell. Specimens (1×2×12 mm, n = 5) of each TPUs were prepared and stretched to failure at a rate of 50 mm/min. The elastic modulus, tensile strength, and ultimate elongation at break were calculated from the resultant engineering stress/strain curves. A secant modulus based on 2% strain was calculated for the elastic modulus and subsequently referred to as the modulus. To test the self-healing properties of light-induced TPU elastomers, the following experimental procedure was employed: Specimens (1×2×12 mm, n = 5) were initially cut to induce damage. The damaged specimens were then exposed to a specific wavelength of light (e.g., UV light) for a set duration to promote self-healing. After the light treatment, the healed specimens were stretched to failure at a rate of 50 mm/min. Engineering stress/strain curves were recorded, and the elastic modulus, tensile strength, and ultimate elongation at break were calculated. Comparing the data before and after light exposure allowed for the evaluation of the self-healing efficacy of the TPU elastomers. Atomic Force Microscopy (AFM) was utilized to characterize the phase behaviors and morphologies of the TPUs. Ultrathin cross-sections of the TPUs were prepared via cryo-ultramicrotomy using a Leica FC7-UC7, and subsequent AFM characterization was performed on a Fastscan AFM from Bruker AXS operating in tapping mode. The AFM images were captured using RTESPA-150 silicon cantilevers, which have a spring constant of 5 $N \cdot m^{-1}$. Differential scanning calorimetry (DSC) measurements were performed using a TA Q2000 instrument, equipped with an electric intracooler as the refrigeration unit. Three samples, each weighing between 5 and 10 mg, were encapsulated in aluminum pans and initially heated from 40 to 220 °C at a rate of 20 °C/min under a constant nitrogen flow to remove any heat history. The samples were then cooled down to -70 °C and subsequently reheated to 220 °C at the same scanning rate of 20 °C/min, again under a steady nitrogen flow. The glass transition temperature (T_g) was determined as the inflection point of the heat capacity change, while the melting temperature (T_m) was identified at the maximum of the endothermic peak, with the area under this peak representing the melting enthalpy. (ΔH_m)[12, 13]. The rheological properties were assessed using an oscillatory rheometer (MCR302, Anton Paar, Graz, Austria) with a 50 mm parallel plate-plate configuration. Prior to testing, film samples with a thickness of approximately 0.3-0.5 mm were prepared and placed between the parallel plates. Relaxation time tests were performed in frequency sweep mode at a strain rate of 5% and a frequency range of approximately 0.1 to 100 Hz at 25 °C.

3. Results & Discussions

3.1. Basic properties of polyurethane elastomers

ATR-IR detailed spectrum is shown in Fig. 5. The absorbance spectrum shows negligible peaks at 2268 cm^{-1}, which is characteristic of the N=C bond in the isocyanate (NCO) functional group in IPDI, while there are distinguished peaks at 3325, 1731, and 1701 cm^{-1} corresponding to the secondary amine N-H, free ester carbonyl, and hydrogen-bonded ester carbonyl stretching bands in the hard segments of TPU. This suggests that IPDI monomers are fully converted to urethane linkages, thereby confirming the successful synthesis of the polyurethane. The TPU was subsequently run through gel permeation chromatography, as demonstrated in Fig. 3. The TPUs' M_w is around 80000 Dal and PDI is 2.5, meeting the TPU's criteria for conducting further experiments.

DOI: 10.54254/2755-2721/130/2025.19994

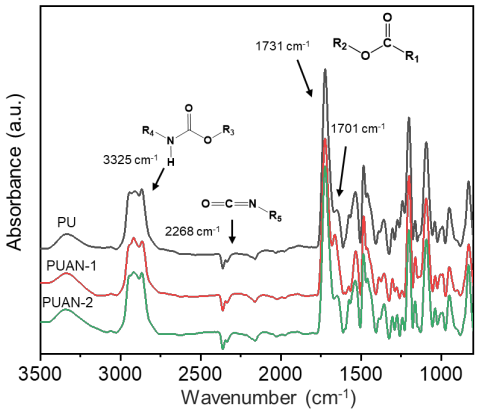

Figure 5: ATR-IR spectra in the range from 1500 to 3500 cm^{-1} for the TPUs.

3.2. Mechanical and Self-healing Properties

The mechanical and self-healing properties are presented in Table 1 and Fig. 6. Among the three groups, PUAN-1 yielded an ultimate tensile strength of 4.4±0.6 MPa, 1165±38.1% elongation at break, and an outstanding 39.7±8.4 MJ/m^3 toughness value. PU, on the other hand, yielded 2.6±0.8 MPa, 978±49.7%, and 22.0±8.8 MJ/m^3 as an ultimate tensile strength, elongation at break, and toughness, while PUAN-2 yielded the worst results of 1.1±0.3 MPa, 959±52.1%, and 9.4±7.4 MJ/m^3 in respective order. Comprehensively reviewing the results of all three groups, it can be observed that incorporating a mild amount of AuNPs, as in PUAN-1, can significantly improve the mechanical properties of the TPU. However, overly incorporating AuNPs in the system, as in PUAN-2, can bring about the exact opposite effect on an ultimate tensile strength and toughness.

Tensile tests were further conducted on PU and PUAN-1 after they were cut and allowed to self-heal to examine their self-healing efficiency. As PUAN-2's mechanical properties were overall unsatisfactory, it was disregarded in the self-healing efficiency test. In alignment with mechanical properties, healing efficiency increased for the group with AuNPs incorporated. For group PUAN-1, the 2 hours of healing resulted in 88.6±16.6%, 93.0±4.3%, and 83.9±26.1% recovery of the UTS, elongation at break, and toughness values compared to the virgin samples. All three values from group PUAN-1 were superior to their corresponding values in group PU, serving as solid evidence that incorporating small amounts of AuNPs can assist with self-healing.

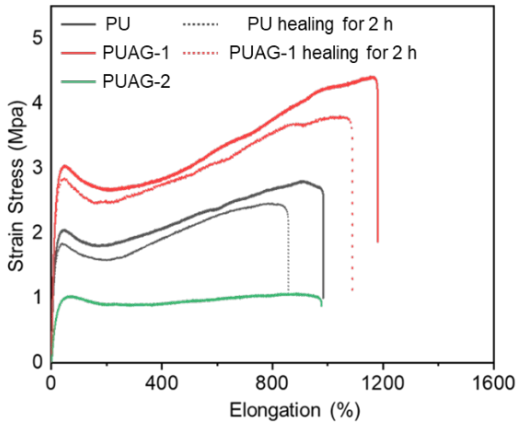

Figure 6: Stress-strain curves for samples.

DOI: 10.54254/2755-2721/130/2025.19994

Table 1: Mechanical properties of samples.

Sample	Young's modulus (Mpa)	Tensile stress (Mpa)	Elongation at break (%)	Toughness (MJ/m3)
PU	16.3±2.1	2.6±0.8	978±49.7	22.0±8.8
PUAN-1	22.1±1.8	4.4±0.6	1165±38.1	39.7±8.4
PUAN-2	4.1±1.9	1.1±0.3	959±52.1	9.4±7.4
PU-healing	14.3±2.4	2.1±1.1	828±55.4	16.9±8.2
PUAN-1-healing	20.4±1.7	3.9±0.5	1084±34.7	33.3±7.6

In general, TPUs with more tightly packed hard segments have better mechanical properties [5, 14, 15], and self-healing efficiency is largely correlated with a polymer's chain mobility [9, 16]. AuNPs' interaction with the TPU network can thus bring about both benefits and downsides, and the balance of the pros and cons determines both self-healing and mechanical attributes. AuNPs possess photothermal properties and can coordinate with disulfide bonds, assisting with disulfide bond reformation; the coordination effect also allows it to serve as the nucleus for hard segment crystallization and thus control hard segment size; AuNPs' crystal nuclei properties can therefore alter the size of the hard segments of the TPUs; their interaction with disulfide bonds can also impair chain mobility. To thoroughly understand both mechanical and self-healing properties, further tests were conducted to confirm the above-mentioned effects of AuNPs on TPU matrices. Chain mobility is essential for the self-healing properties of TPUs. To assess chain mobility, a frequency sweep test was performed on all three samples. The relaxation time (λ), which indicates the recovery time from external mechanical stresses, serves as a reliable measure of self-healing efficiency, reflecting chain mobility within similar polymers[10, 16]. The relationship between λ and the frequency of application of mechanical stress is demonstrated in the frequency sweep graph in Fig. 7. PU is shown to have the lowest λ among the three groups over the entire range of frequencies, followed by PUAN-1 and PUAN-2. This presents strong evidence that progressively incorporating AuNPs would increasingly impair polymer chains' mobility. Provided that PUAN-1 has higher self-healing efficiency, however, it is likely that AuNPs' photothermal properties and coordination with disulfide bonds made up for the impeded chain mobility [17-20]. Furthermore, despite no self-healing tests being conducted on PUAN-2, it can be well guaranteed to have low self-healing efficiency. Although the relationship between AuNPs and chain mobility has been uncovered, in what approach do AuNPs block chain motion is not exactly unknown, and that is up to further testing to unveil.

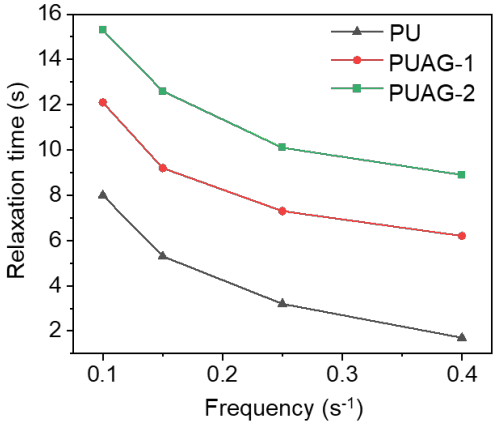

Figure 7: Plots of relaxation time (λ) versus frequency at 25 °C of the TPUs.

DOI: 10.54254/2755-2721/130/2025.19994

3.3. Topography and structure of polyurethane elastomers

The mechanical properties of TPUs varied drastically in the tensile experiment. To understand the behavior of the TPU samples from a molecular perspective, the acquired ATR-FTIR data, specifically the region from 1800 to 1600 cm^{-1} corresponding to ester ketones, was processed through peak splitting as shown in Fig.8. Carbonyl group within the TPU network can adopt four distinct forms: (1) Carbonyl group with a wavenumber around 1800 cm^{-1} correspond to free carbonyls, (2) ~1730 cm^{-1} corresponds to hydrogen-bonded but unstructured carbonyls, (3) ~1700 cm^{-1} corresponds to hydrogen-bonded and structured carbonyls (crystallized carbonyls in hard segments), (4) ~1650 to crystallized carbonyls in soft segments[21]. As the content of hydrogen-bonded and structurally regular carbonyls indicates how tightly packed the hard segments of the TPU are, the latter positively correlated with the TPU's mechanical robustness, the underlying reason accounting for the difference in strength across the three groups can be preliminarily determined by comparing the percentage of carbonyls around 1700 cm^{-1} [21]. The detailed peak-splitting data are summarized in Table 2. From the data, the content of tightly packed hard segments can be ranked in the order PUAN-1 > PUAN-2 > PU. It can be validated from the order that AuNPs increase tightly packed hard segment content, confirming the hypothesis that AuNPs can serve as crystal nuclei to assist with hard segment crystallization. The results align with the outcomes of the conventional tensile test in that group PUAN-1, the group with the highest content of tight hard segments, shows the best mechanical strength, and likely substantiates that PUAN-1's mechanical robustness partially results from its high proportion of tightly packed hard segments. However, group PUAN-2, the group with the worst results from the tensile experiments, has the second-highest content of tightly packed hard segments. The contradiction can be accounted for in that FTIR peak splitting can only demonstrate the proportional content of the hard segments but cannot illustrate the conditions of the hard segments; that is, hard segments may be abundant in the TPU matrices of PUAN-2 samples, but the physical structure of the hard segments cannot be determined solely from the peak splitting data. For instance, if the hard segments are small, they may not provide adequate mechanical support against tensile stresses.

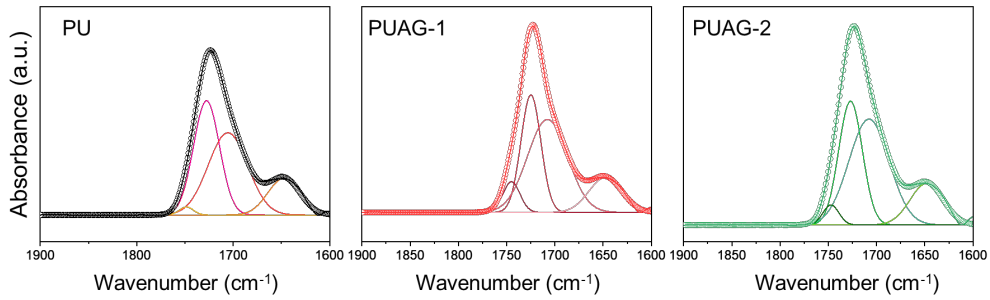

Figure 8: ATR-IR spectra in the range from 1500 to 3500 cm^{-1} for the TPUs.

Table 2: The calculated area percentages (area%) of the corresponding bands in the ATR-IR spectra for samples.

Sample	Band I (% area ~1800 cm^{-1})	Band II (% area ~1730 cm^{-1})	Band III (% area ~1700 cm^{-1})	Band IV (% area ~1650 cm^{-1})
PU	1.5	39.3	43.6	15.7
PUAN-1	1.6	29.0	60.9	10.5
PUAN-2	4.7	30.4	53.0	13.9

DOI: 10.54254/2755-2721/130/2025.19994

To seek more information about the physical structure of the TPUs, DSC tests were conducted over the temperature range of -50 to 200℃. All three groups demonstrated typical patterns of glass transition over the range of -25 to 0℃. T_g can be ranked with the order PUAN-2 > PUAN-1 > PU. As T_g is inversely correlated with the degree of microphase separation in the TPU matrix, that is, a higher T_g indicates a lower extent of microphase separation[22], increasing AuNP content also led to decreasing microphase separation. This is consistent with the frequency sweep test in that a lower level of microphase separation would lead to more hard segments incorporated into the soft segments, handicapping the mobility of soft segments. Upon scrutinizing the very end of the DSC curve around 175℃, however, only group PUAN-1 demonstrated a somewhat recognizable T_m. As T_m is the temperature at which the crystallized hard segments in TPU matrices melt, or the temperature at which their tight hydrogen bonding structure is dismantled, it can be shown that PUAN-1 has the most tightly packed hard segments that T_m can be spotted on its curve. This resonates with peak splitting data, serving as further evidence that AuNPs strengthened hard segments and thus enhanced TPUs' mechanical properties. This also exemplifies that hard segment crystallization is carried out better with a milder amount of AuNPs; however, the exact reason for that must be confirmed with atomic force microscopy (AFM), which most directly displays the physical structure of the TPUs.

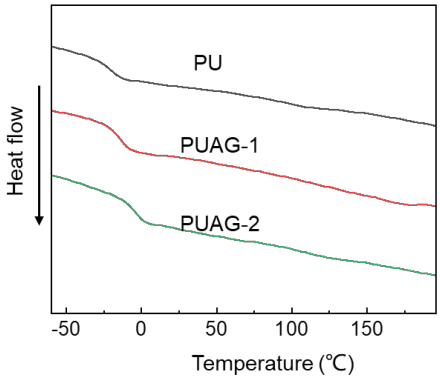

Figure 9: DSC results of the TPUs.

As a most direct method for observing the internal structure of the TPUs and deducing the effect of AuNP on the physical structure of TPU matrices, AFM was conducted. The detailed AFM images are displayed in Fig. 10. In the AFM images, hard segments are displayed as bright areas (including bright clusters and brighter orange sections), soft segments as lighter dark sections, and crystallized soft segments likely as white dots. Directly, it can be validated that microphase separation does decrease with AuNPs incorporated, as the area of bright domains in the soft domain visibly increased from PU to PUAN-2, linking back to the trend of DSC T_g temperatures and chain mobility trend. This is likely due to some amounts of AuNPs failing to crystallize into larger hard segments, thus embedding in the soft segments. Moreover, the number of hard segments notably increases with the amount of AuNPs in the matrix, further pointing to the speculation that AuNPs can serve as crystal nuclei and aid hard segment crystallization. The ability of AuNPs to control hard segment size is also confirmed: with a moderate amount of AuNPs in PUAN-1, hard segments are more centralized to form small amounts of large clusters that are evenly distributed, while with a large amount as in PUAN-2, many tightly packed hard segments are smaller-sized and scattered, and few hard segments are way oversized. Under AuNP intervention, hard segments surround the AuNP to construct a compact hard domain, hence fewer AuNPs would create fewer but larger domains, and vice versa. The size and distribution of the hard segments also provided clues about the TPUs' mechanical properties. In a mechanism aspect, when a TPU matrix encounters a stretching force, the mobile soft segments rely on tightly packed hard segments for mechanical support. With hard segments being

DOI: 10.54254/2755-2721/130/2025.19994

reasonably large, tightly packed, and finely distributed over the TPU matrix, the external force can be well dispersed, and the material has less tendency to break. On the other hand, if hard segments are small or excessively large, they either cannot provide support against the stretch force or the force will be centralized to a few points, accelerating the material's failure. The well-sized and evenly dispersed hard segments in PUAN-1 explain its mechanical potency, and the combination of unusually small and large hard segments in PUAN-2 justifies its unsatisfactory stress-enduring ability.

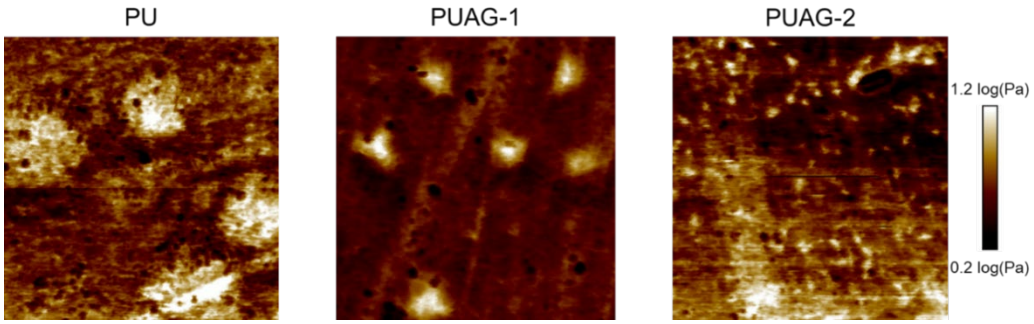

Figure 10: AFM phase images of the TPUs.

Hence, a moderate amount of AuNPs can interact with the disulfide bonds in the hard segments of polyurethane, acting as a reinforcing phase to enhance the mechanical properties of TPU. However, an excessive amount of AuNPs can excessively interact with the disulfide bonds, restricting the mobility of polyurethane molecular chain segments and inhibiting microphase separation, resulting in a decline in TPU's mechanical properties. Regarding self-healing performance, a suitable amount of AuNPs can facilitate the dynamic exchange of disulfide bonds in the hard segments due to their photothermal properties, converting light energy into heat. This promotes self-healing. In contrast, an excessive amount of AuNPs restricts the mobility of polyurethane chain segments and inhibits self-healing, leading to a decrease in TPU's self-healing efficiency.

4. Conclusion

In summary, we developed an easily processable TPU (PUAN-1) with quick self-healing ability and outstanding stretchability and robustness. The core of the TPU's distinction is the incorporation of AuNPs, which enhanced the TPU's mechanical attributes and healing efficiency by strengthening its hard segments and assisting with disulfide bond reformation through coordination and photothermal effects. Based on the exceptional quality of the TPU, we hold confidence that it is a promising material for applications requiring durable and self-repairing components, such as wearable electronics, flexible sensors, and biomedical devices. The TPU's ability to recover quickly from damage while maintaining high mechanical performance makes it ideal for use in dynamic environments where both strength and longevity are critical.

References

[1] *Karna, N.; Joshi, G. M.; Mhaske, S. T. Structure-property relationship of silane-modified polyurethane: A review. Progress in Organic Coatings 2023, 176, 107377. DOI: https://doi.org/10.1016/j.porgcoat.2022.107377.*

[2] *Yilgor, I.; Eynur, T.; Yilgor, E.; Wilkes, G. L. Contribution of soft segment entanglement on the tensile properties of silicone–urea copolymers with low hard segment contents. Polymer 2009, 50 (19), 4432-4437. DOI: https://doi.org/10.1016/j.polymer.2009.07.016.*

[3] *Mannsfeld, S. C. B.; Tee, B. C. K.; Stoltenberg, R. M.; Chen, C. V. H. H.; Barman, S.; Muir, B. V. O.; Sokolov, A. N.; Reese, C.; Bao, Z. Highly sensitive flexible pressure sensors with microstructured rubber dielectric layers. Nature Materials 2010, 9 (10), 859-864. DOI: 10.1038/nmat2834.*

[4] Wu, Y.; Liu, C.; Lapiere, M.; Ciatti, J. L.; Yang, D. S.; Berkovich, J.; Model, J. B.; Banks, A.; Ghaffari, R.; Chang, J.-K.; et al. Thermoplastic Elastomers for Wireless, Skin-Interfaced Electronic, and Microfluidic Devices. ADVANCED MATERIALS TECHNOLOGIES 2023, 8 (19), Article. DOI: 10.1002/admt.202300732 (acccessed 2023-08-05).

[5] An, Z.-W.; Xue, R.; Ye, K.; Zhao, H.; Liu, Y.; Li, P.; Chen, Z.-M.; Huang, C.-X.; Hu, G.-H. Recent advances in self-healing polyurethane based on dynamic covalent bonds combined with other self-healing methods. Nanoscale 2023, 15 (14), 6505-6520, Review. DOI: 10.1039/d2nr07110j.

[6] Aguirresarobe, R. H.; Nevejans, S.; Reck, B.; Irusta, L.; Sardon, H.; Asua, J. M.; Ballard, N. Healable and self-healing polyurethanes using dynamic chemistry. Progress in Polymer Science 2021, 114, 101362.

[7] Li, W.; Wu, H.; Huang, Y.; Yao, Y.; Hou, Y.; Teng, Q.; Cai, M.; Wu, J. Ultra-Fast-Healing Glassy Hyperbranched Plastics Capable of Restoring 26.4 MPa Tensile Strength within One Minute at Room Temperature. Angew. Chem. Int. Ed. 2024. DOI: 10.1002/anie.202408250.

[8] Li, Y.; Zhou, M.; Wang, R.; Han, H.; Huang, Z.; Wang, J. Self-healing polyurethane elastomers: An essential review and prospects for future research. Eur. Polym. J. 2024, 214, Article. DOI: 10.1016/j.eurpolymj.2024.113159 (acccessed 2024-06-22).

[9] Li, B.; Cao, P.-F.; Saito, T.; Sokolov, A. P. Intrinsically Self-Healing Polymers: From Mechanistic Insight to Current Challenges. CHEMICAL REVIEWS 2023, 123 (2), 701-735, Review. DOI: 10.1021/acs.chemrev.2c00575 (acccessed 2023-01-15).

[10] Eom, Y.; Kim, S.-M.; Lee, M.; Jeon, H.; Park, J.; Lee, E. S.; Hwang, S. Y.; Park, J.; Oh, D. X. Mechano-responsive hydrogen-bonding array of thermoplastic polyurethane elastomer captures both strength and self-healing. Nature Communications 2021, 12 (1), 621.

[11] Ma, J.; Deng, B.; Fan, Y.; Huang, X.; Chen, D.; Ma, Y.; Chen, H.; Grzesiak, A. L.; Feng, S. Polyurethane elastomers with amphiphilic ABA tri-block co-polymers as the soft segments showing record-high tensile strength and simultaneously increased ductility. Polymer Chemistry 2022, 13 (35), 5159-5168, 10.1039/D2PY00752E. DOI: 10.1039/D2PY00752E.

[12] Krol, P. Synthesis methods, chemical structures and phase structures of linear polyurethanes. Properties and applications of linear polyurethanes in polyurethane elastomers, copolymers and ionomers. Prog. Mater Sci. 2007, 52 (6), 915-1015. DOI: 10.1016/j.pmatsci.2006.11.001.

[13] Zhu, Y.; Hu, J.; Yeung, K. Effect of soft segment crystallization and hard segment physical crosslink on shape memory function in antibacterial segmented polyurethane ionomers. Acta Biomaterialia 2009, 5 (9), 3346-3357. DOI: 10.1016/j.actbio.2009.05.014.

[14] Xu, J.; Li, Y.; Liu, T.; Wang, D.; Sun, F.; Hu, P.; Wang, L.; Chen, J.; Wang, X.; Yao, B.; et al. Room-Temperature Self-Healing Soft Composite Network with Unprecedented Crack Propagation Resistance Enabled by a Supramolecular Assembled Lamellar Structure. Adv. Mater. 2023, 35 (26), 2300937. DOI: https://doi.org/10.1002/adma.202300937.

[15] Kang, J.; Tok, J. B. H.; Bao, Z. Self-healing soft electronics. NATURE ELECTRONICS 2019, 2 (4), 144-150, Review. DOI: 10.1038/s41928-019-0235-0 (acccessed 2019-04-01).

[16] Kim, S.-M.; Jeon, H.; Shin, S.-H.; Park, S.-A.; Jegal, J.; Hwang, S. Y.; Oh, D. X.; Park, J. Superior Toughness and Fast Self-Healing at Room Temperature Engineered by Transparent Elastomers. Adv. Mater. 2018, 30 (1), 1705145. DOI: https://doi.org/10.1002/adma.201705145 (acccessed 2024/08/20).

[17] Xing, R.; Liu, K.; Jiao, T.; Zhang, N.; Ma, K.; Zhang, R.; Zou, Q.; Ma, G.; Yan, X. An Injectable Self-Assembling Collagen-Gold Hybrid Hydrogel for Combinatorial Antitumor Photothermal/Photodynamic Therapy. ADVANCED MATERIALS 2016, 28 (19), 3669-3676, Article. DOI: 10.1002/adma.201600284 (acccessed 2016-05-18).

[18] Guo, H.; Han, Y.; Zhao, W.; Yang, J.; Zhang, L. Universally autonomous self-healing elastomer with high stretchability. NATURE COMMUNICATIONS 2020, 11 (1), Article. DOI: 10.1038/s41467-020-15949-8 (acccessed 2020-05-18).

[19] Xu, Y.; Zhou, S.; Wu, Z.; Yang, X.; Li, N.; Qin, Z.; Jiao, T. Room-temperature self-healing and recyclable polyurethane elastomers with high strength and superior robustness based on dynamic double-crosslinked structure. Chem. Eng. J. 2023, 466, Article. DOI: 10.1016/j.cej.2023.143179 (acccessed 2023-05-28).

[20] Zhang, Q.; Duan, J.; Guo, Q.; Zhang, J.; Zheng, D.; Yi, F.; Yang, X.; Duan, Y.; Tang, Q. Thermal-Triggered Dynamic Disulfide Bond Self-Heals Inorganic Perovskite Solar Cells. ANGEWANDTE CHEMIE-INTERNATIONAL EDITION 2022, 61 (8), Article. DOI: 10.1002/anie.202116632 (acccessed 2022-01-18).

[21] Rueda-Larraz, L.; d'Arlas, B. F.; Tercjak, A.; Ribes, A.; Mondragon, I.; Eceiza, A. Synthesis and microstructure–mechanical property relationships of segmented polyurethanes based on a PCL–PTHF–PCL block copolymer as soft segment. Eur. Polym. J. 2009, 45 (7), 2096-2109. DOI: https://doi.org/10.1016/j.eurpolymj.2009.03.013.

[22] Cheng, B.-X.; Gao, W.-C.; Ren, X.-M.; Ouyang, X.-Y.; Zhao, Y.; Zhao, H.; Wu, W.; Huang, C.-X.; Liu, Y.; Liu, X.-Y.; et al. A review of microphase separation of polyurethane: Characterization and applications. Polym. Test. 2022, 107. DOI: 10.1016/j.polymertesting.2022.107489.